energy&fuels

Article

pubs.acs.org/EF

Effect of Hydrate Formation Conditions on Thermal Conductivity of Gas-Saturated Sediments

Evgeny Chuvilin*[,†,‡] and Boris Bukhanov[†]

[†]Skolkovo Institute of Science and Technology (Skoltech), 3 Nobel Street, Skolkovo Innovation Center, Moscow 143026, Russia
[‡]Geology Faculty, Moscow State University (MSU), 1 Leninskie Gory, GSP-1, Moscow 119991, Russia

ABSTRACT: The paper summarizes experimental data on thermal conductivity variations in gas-saturated sediments exposed to hydrate formation at various conditions. All experiments were performed on a specially designed gas hydrate system maintaining a high gas pressure and a steady-state thermal regime, with a built-in unit for thermal conductivity measurements. The measurements were applied to natural samples of fine sand and silty sand collected from gas emanation sites in permafrost and to artificial sand and sand−clay mixtures. The results show that thermal conductivity can either increase or decrease depending upon hydrate formation conditions. Namely, it increases if gas hydrates form at positive temperatures ($t > 0$ °C) but decreases during hydrate formation in frozen samples. Freezing and thawing of hydrate-bearing sediments above the equilibrium pressure reduce their thermal conductivity as a result of additional hydrate formation. Experimental results are used to model hydrate and ice formation in gas-saturated sediments. The experimental study of thermal conductivity in hydrate-bearing sediments has implications for simulations of methane recovery from natural gas hydrate reservoirs and the respective technologies.

INTRODUCTION

Natural gas hydrates (mainly hydrates of methane) often form in marine sediments at depths below 300 m or in soil beneath permafrost.[1−3] Sediments exposed to long-term freezing cool over hundreds of meter depths, whereby gas-bearing strata fall into the zone of hydrate stability and gas hydrates form before the freezing front. Note that thickening of permafrost leads to the formation of naturally frozen hydrate-bearing soils. Hydrates mostly form at great depths or can also be found at shallow depths (within 250 m) in high-temperature permafrost. Permafrost is subject to high pressures from crystallization of pore water (crystallization factor) and from loads applied to gas pockets in frozen sediments (baric factor).[4,5] The baric factor is mainly associated with transgression of the Arctic seas and glaciation.[6] As a result, gas accumulated at relatively shallow depths in permafrost enters the zone of hydrate stability and transforms into hydrate. Thus, hydrate can also form beneath permafrost at low positive temperatures and subzero temperatures in permafrost.

According to the available estimates of natural gas hydrate resources,[7,8] the amount of methane sequestered in hydrates is orders of magnitude greater than that in conventional and unconventional gas reservoirs taken together. Makogon et al.[7] estimated it to be 7.6×10^{18} m^3, assuming that hydrates can occur wherever the conditions for their formation and stabilization exist. However, this may be an overestimated amount, judging by more recent *in situ* field data. The most conservative recent estimate by Johnson[8] is 3×10^{15} m^3. According to Boswell and Collet,[9] technically recoverable volume of gas in gas hydrate reservoirs is approximately 3×10^{13} m^3. There exist several methods for methane recovery from hydrate resevoirs: depressurization, thermal stimulation, inhibitor injection, and carbon dioxide (CO_2) replacement or combinations of these techniques.[10−12] It is crucial to use actual thermal conductivities of hydrate-bearing sediments in simulations for choosing the best development strategy.[13] Methane production from hydrate reservoirs is most often simulated with reference to thermal conductivity of pure methane hydrates,[14] but this assumption neglects the specificity of hydrate reservoirs and entrains serious errors during methane recovery, especially for permafrost that contains hydrates and ice.

Thermal conductivity is known to be different in pore water and ice (0.6 and 2.23 W m^{-1} K^{-1}, respectively) but similar in water and gas hydrate (0.6 and 0.55−0.65 W m^{-1} K^{-1}, respectively).[15−18] Therefore, thermal conductivity variations during pore hydrate formation in sediments presumably depend upon the conditions. The thermal conductivity of hydrate-bearing sediments has been worse studied than that of pure gas hydrate, with the available data being restricted to sporadic estimates for artificial hydrate-bearing sediments reported by Groysman,[19] Asher,[20] Fan et al.,[21] Waite et al.,[17] Duchkov et al.,[22] Muraoka et al.,[23] and Yang et al.[24]

The first experimental evidence on thermal conductivity of sediments containing natural gas hydrates was obtained from well Malik 5L-38 (Mackenzie Delta, Canada).[25] Frozen soils were found to have thermal conductivity generally higher than their hydrate-bearing frozen counterparts. On the other hand, hydrate-saturated sediments are often more thermally conductive in a frozen state than an unfrozen state. New experimental data on thermal conductivity of natural gas hydrate-bearing sediments from the Nankai Trough, published a few years ago,[26] were used to predict thermal conductivity from the known particle size distribution, porosity, and hydrate saturation of sediments. A complex distribution model (geometric mean model) provided the most successful

Received: October 19, 2016
Revised: January 27, 2017
Published: March 27, 2017

DOI: 10.1021/acs.energyfuels.6b02726
Energy Fuels 2017, 31, 5246−5254

prediction for natural sediments with hydrate saturation under 14%, but the proposed equations were poorly applicable to sediment samples containing greater percentages of hydrates (up to 30%).[23] The reason is mainly that hydrate-bearing sediments are complex systems, in which thermal conductivity also depends upon their structure and texture, especially on contacts between particles, rather than being a mere sum of thermal conductivity values of the system constituents.

The thermal conductivity of frozen hydrate-saturated sediments was studied by Bukhanov et al.[27] under non-equilibrium conditions, i.e., during self-preservation of methane hydrates. The authors reported a method for thermal conductivity estimation and confirmed that frozen sediments with and without hydrates differed in thermal conductivity on account of self-preservation (anomalous preservation) of porous gas hydrates below 0 °C and 0.1 MPa.[28,29]

The knowledge gaps concerning thermal conductivity of gas hydrate-bearing sediments result mainly from overlooking the issues of their structure, texture, and pore space. Thus, it is important to investigate experimentally the thermal conductivity of sediments at low positive (above 0 °C) and slightly negative (below 0 °C) temperatures as a function of the hydrate saturation and amount of pore water converted into hydrate. We present a summary of the respective experimental results obtained at different conditions of gas hydrate formation and use these results for reference to model structural and textural changes in gas-saturated sediments under different conditions of hydrate formation, including freezing and thawing.

METHOD

Thermophysical studies of porous gas hydrates were performed using a specially designed system for measuring thermal conductivity of porous materials in a pressure cell under different temperatures and pressures. The setup includes a refrigerator maintaining the preset temperature of samples, a gas hydrate cell (200 cm^3 total volume), a gas bomb (300 cm^3), tubes, power supplies (12 V for the cooler and 20 V for the heater), thermistors, an analog to digital converter (ADC), and a personal computer (PC) (Figure 1). The gas hydrate

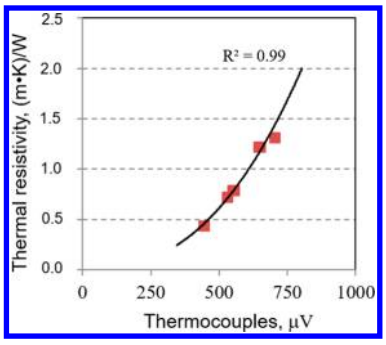

Figure 1. Calibration curve for estimating thermal conductivity of gas-saturated sediments. Red squares are reference data points with known thermal conductivity. The line is an approximation curve for readings of thermocouples.

cell, consisting of two metal cylinders (one inside another), contains an in-built unit for thermal conductivity measurements in fine-grained samples, which was designed in collaboration with colleagues from the Nature Management Institute at the National Academy of Sciences of Belarus (Minsk, Belarus). The thermal conductivity of samples was measured in a steady-state mode[30] at the temperature difference between two ends of the samples kept constant by a constant-power 1 W heater (red in Figure 1). As estimated empirically, transition to the steady-state mode caused 0.8−1.2 °C overheating of samples. A protective heater and thermocouples were installed additionally on the bottom of the inner cylinder to prevent heat loss from the main heater. Thermal conductivity measurements with this system were accurate to 7%, with 0.95 confidence and with a random error not exceeding 4%.[31] The desired accuracy during calibration was monitored and maintained using thermal pastes as reference materials, with known thermal conductivities in the range of 0.76−2.23 W m^{-1} K^{-1} (Figure 2), measured in the steady-state mode to an absolute error of 5%, according to ASTM recommendations.[32]

The measurements were applied to synthetic (model) and natural samples with a deformed structure (Table 1). The model samples were quartz sand (sand-1) and a sand−clay mixture of sand-1 and 14% kaolin clay. The natural samples were poly mineral sand (sand-2) and poly mineral silty sand from gas-saturated permafrost in Russia.

The methane pressure in the cell was maintained above equilibrium in all experiments to prevent dissociation of pore gas hydrate during thermal conductivity measurements. Calculations show that errors associated with possible phase transitions during thermal conductivity measurements are very small and cause no effect on the results because of low power of the heater and constant temperature and pressure monitoring. The initial values of density (ρ) and porosity (n) of the samples were within 1.7−1.9 g/cm^3 and 0.38−0.45, respectively, in all runs. Additionally, lower density samples were prepared with the initial parameters $n \sim 0.6$ and ρ = 1.3−1.4 g/cm^3. Hydrate formation was with methane (99.98%) stored in a bomb at a pressure of ∼8−10 MPa. The behavior of thermal conductivity of sediments at above-equilibrium methane pressure was studied at positive and negative temperatures.

The experiments included several steps: (1) methane injection (6.0 MPa) to the pressure cell with samples at room temperature ($t \approx 21 \pm 1$ °C) and subsequent cell cooling to +2 ± 1 °C, (2) hydrate saturation at +2 ± 1 °C and methane pressure above 4.2 MPa (maintaining methane pressure above equilibrium ensures hydrate formation in all samples), and (3) freezing of the gas hydrate-bearing sample ($t \approx -5$, ..., −8 °C), while the residual pore water not converted to hydrate freezes and induces additional hydrate formation.[30] In the latter case, thermal conductivity was studied at a constant negative temperature of −5 ± 1 °C and subsequent thawing at a low positive temperature. At low temperatures (−5 ± 1 °C), hydrate formation from pore ice started immediately after cooled methane (at 6 MPa) had saturated the pressure cell with the frozen sample. After hydrate had formed at a preset negative temperature, the pressure cell with the sample was heated to a positive temperature (t = +2 ± 1 °C), while the pressure was still maintained above equilibrium. As a result, additional hydrate formed as the sample heated and thawed. At each step, pressure, temperature, and thermal conductivity of samples were measured. For comparison, the same parameters were measured under atmospheric pressure and at 3−4 MPa created by nitrogen (N_2), which did not form hydrate under the run conditions.

The pressure, volume, and temperature (PVT) method under varied thermobaric conditions was used to determine the volume content of hydrate (H_v, %), hydrate saturation (S_h, %), and fraction of water changed to hydrate (K_h, unit fraction),[33] given by

$$H_v = \frac{M_h \rho}{M_s \rho_h} \times 100\% \quad (1)$$

where M_h is the weight of the pore gas hydrate (g), M_s is the weight of the sample (g), ρ is the sample density (g/cm^3), and ρ_h is the hydrate density. ρ_h was assumed to be 0.794 g/cm^3 for CH_4 hydrates, as crystallographic density of an empty square lattice (without gas molecules by analogy with the pure ice structure), and based on experimental data by Takeya et al.[34]

$$S_h = \frac{H_v}{n} \quad (2)$$

where n is the porosity of sediment samples

DOI: 10.1021/acs.energyfuels.6b02726
Energy Fuels 2017, 31, 5246−5254

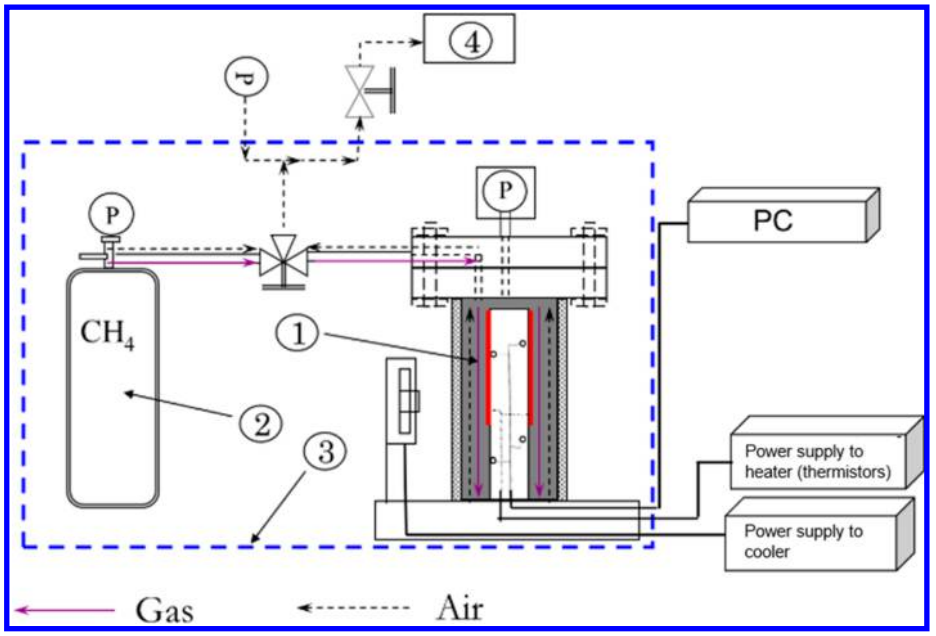

Figure 2. System for measuring thermal conductivity of sediment samples under gas pressure, with a general layout: (1) gas hydrate cell with a sample inside, (2) gas bomb, (3) refrigerator, and (4) vacuum pump.

Table 1. Properties of Samples

	grain size fraction (%)					
sample (sediment type)	1−0.05 mm	0.05−0.001 mm	<0.001 mm	mineralogy (%)		salinity (%)
sand-1	94.8	3.1	2.1	quartz	>90	0.01
sand-2	82.3	12.7	2.7	quartz	54	0.40
				microcline + albite	42	
				illite	4	
silty sand	41.8	53.7	4.5	quartz	37	0.08
				microcline + albite	55	
				illite	8	
kaolin	4.5	70.9	24.6	kaolinite	92	0.04
				quartz	6	
				muscovite	2	

$$K_h = \frac{W_h}{W} \quad (3)$$

where W_h is the amount of water converted to hydrate (% of dry sample weight) and W is the total amount of water (initial water content, %).

The hydrate content in sediments containing methane hydrates was calculated using hydrate number 5.9.[33,35]

EXPERIMENTAL DATA AND DISCUSSION

Variations in thermal conductivity of samples were analyzed at different conditions of hydrate formation: (1) low positive temperatures ($t \approx +2 \pm 1$ °C), (2) negative temperatures ($t \approx -5 \pm 1$ °C), (3) cooling from $+2 \pm 1$ to from -5 to -8 °C, where residual pore water (not changed to hydrate at positive temperatures) froze and induced additional hydrate formation, and (4) warming from -5 ± 1 to $+2 \pm 1$ °C, where residual pore ice (not changed to hydrate at negative temperatures) thawed and induced additional hydrate formation.

The influence of the hydrate formation conditions on the thermal properties was studied in sand−silt samples not fully saturated by water or ice.

Hydrate Formation at $t > 0$ °C. To investigate hydrate formation at $t > 0$ °C in the pressure cell, undersaturated methane-bearing samples were cooled from room to low positive ($t = +2 \pm 1$ °C) temperatures. The typical pattern of gas hydrate formation in pores of samples exposed to cooling is evident in time-dependent variations in the fraction of water converted to hydrate, K_h (Figure 3a). This fraction decreases with time as a result of changes in the hydrate formation mechanism. Hydrate formation is rapid early during the process, and most of hydrate forms within the first 45−50 h, consuming about 45% of pore water (Figure 3a), while H_v (Figure 3b) and S_h (Figure 3c) reach 22 and 67%, respectively. Then, hydrate formation decelerates, while K_h, H_v, and S_h remain almost invariable (0.46, 27%, and 67%, respectively). The closely correlated volume content of hydrate (H_v, %), the portion of pore space filled with hydrate (S_h, %), and the fraction of water converted to hydrate (K_h, unit fraction) are the main focus of this study.

The observed kinetics of hydrate formation at low positive temperatures can be explained as follows. Rapid formation of hydrates in the beginning is due to well-developed gas−water contacts. Later, a gas hydrate film forms at the pore water−gas interface and impedes gas access to pore water, whereby the hydrate formation rate slows, being limited by the permeability of the gas hydrate film. The thickening of the hydrate film

DOI: 10.1021/acs.energyfuels.6b02726
Energy Fuels 2017, 31, 5246−5254

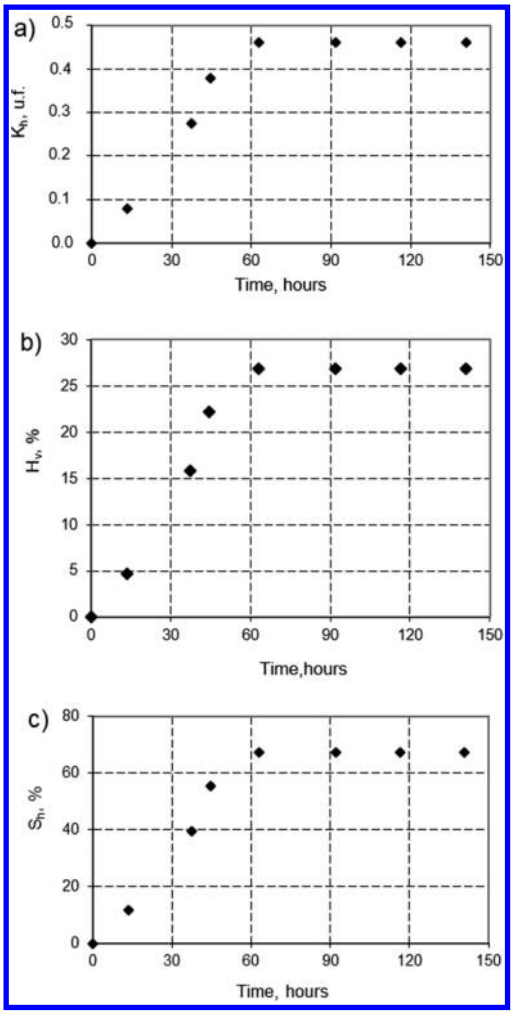

Figure 3. Pore hydrate formation in gas-saturated silty sand (W = 18%; n = 0.40), at t = +2 ± 1 °C: (a) time-dependent fraction of water changed to hydrate (K_h, unit fraction), (b) volume content of hydrate (H_v, %), and (c) hydrate saturation (S_h, %).

makes it much less permeable, and hydrate formation almost stops at a certain film thickness, despite the fact that the residual pore water content exceeds the equilibrium water content at given temperatures and pressures.

The time-dependent thermal conductivity of gas-saturated silty sand (W = 18%) during hydrate accumulation at positive temperatures shows an irregular behavior (Figure 4), with three characteristic regions in the plot. For the first 40 h, thermal

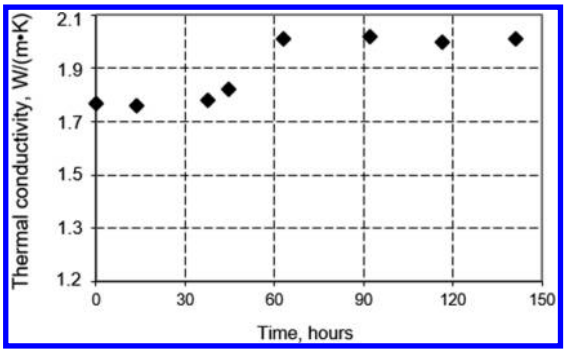

Figure 4. Time-dependent thermal conductivity of gas-saturated silty sand (W = 18%; n = 0.40) during hydrate formation at t = +2 ± 1 °C.

conductivity changes from 1.77 to 1.78 W m^{-1} K^{-1} or within a measurement accuracy of 3%. Then, it increases from 1.78 to 2.01 W m^{-1} K^{-1} or for 13% for the following 20 h and remains almost invariable about 2.01 W m^{-1} K^{-1}, likewise within a measurement accuracy (3−4%) after 60 h from the run start.

As for hydrate formation in silty sand (W = 18%), S_h becomes 40% higher for the first 40 h, while thermal conductivity almost does not change, and then both parameters increase for the following 20 h, peak concurrently, and remain invariable within 100 h afterward. However, thermal conductivity does not change at gas saturation S_h < 45% (Figure 5), as other authors reported previously.[23,25,26] The variations become notable when hydrates occupy more than 45% of pore space. Thus, thermal conductivity became 14% higher, while S_h reached 61% in silty sand with W = 18% and 9% higher as S_h increased to 57% in sand-1.

Hydrate Formation at t < 0 °C. Hydrate formation at t < 0 °C was studied in frozen methane-bearing samples in the same pressure cell, at temperatures of −5 ± 1 °C (Figure 6). Unlike the tests at low positive temperatures, methane hydrates form more slowly at negative temperatures. As a result, the rate of hydrate formation in frozen samples is commensurate with that at positive temperatures[36] for quite a long time. The reason is that, at negative temperatures, gas hydrates form directly on the surface of ice particles, as demonstrated by special studies of interaction between ice particles and CO_2 and CH_4 gases.[33,37−39] Hydrate that forms during this interaction has a low density and, hence, a high permeability and does not impede much for the conversion of ice particles to hydrate. The same mechanism apparently works during transition of pore ice into hydrate, judging by the dynamics of gas hydrate formation in frozen sediments.

Unlike the case of t > 0 °C, the thermal conductivity of frozen samples decreases non-uniformly with time during hydrate formation (Figure 7). The decrease is to 1.81 W m^{-1} K^{-1} (8%) for the first 50 h of hydrate growth and then as small as 3% for the subsequent 125 h. In general, this decrease is observed in the S_h range from 0 to 50−60% (Figure 8). The thermal conductivity decrease most likely results from reduction in the amount of ice, with its thermal conductivity as high as 2.23 W m^{-1} K^{-1}, and the related growth in the share of the less conductive hydrate (0.6 W m^{-1} K^{-1}).

Effect of Freezing. To study the effect of freezing on thermal conductivity variations, the samples saturated with hydrate at t > 0 °C were cooled from −5 to −8 °C. Although hydrate had already saturated 50−60% of pore space before freezing and hydrate formation almost ceased, further cooling of the samples led to the formation of additional hydrate in all runs (Table 2).

Thus, the hydrate saturation increase (ΔS_h) was around 23−28% for sand and 39−52% for silty sand samples, where

$$\Delta S_h = \frac{S_h^{\text{before freezing}} - S_h^{\text{after freezing}}}{S_h^{\text{before freezing}}} \times 100\% \quad (4)$$

Thus, more hydrate formed in silt than in sand upon freezing. The same tendency was observed in the sand−clay samples: a 5% greater amount of additional hydrate formed in sand with 14% kaolin clay (W = 16%) than in pure sand (sand-1).

Thus, a large portion of water that survived conversion to hydrate at positive temperatures became consumed during cooling and freezing. Hydrate formation became more active as the surviving pore water froze because cryotic deformation of

DOI: 10.1021/acs.energyfuels.6b02726
Energy Fuels 2017, 31, 5246−5254

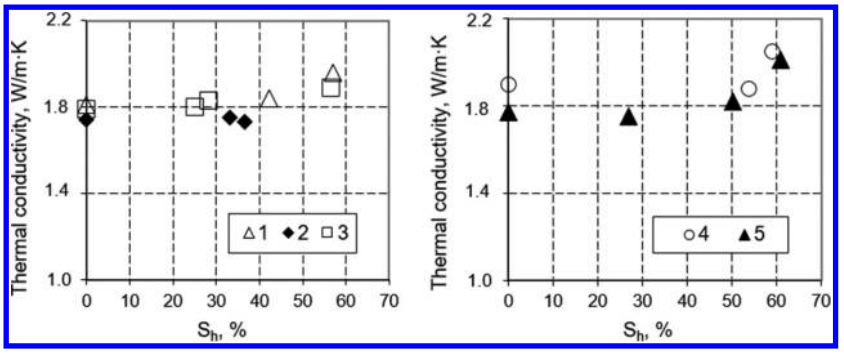

Figure 5. Thermal conductivity of sediments as a function of hydrate saturation (S_h) at t = +2 ± 1 °C: (1) sand-1, W = 16%; (2) sand-1, W = 10%; (3) sand-2, W = 15%; (4) sand + 14% kaolin clay, W = 15%; and (5) silty sand, W = 18%.

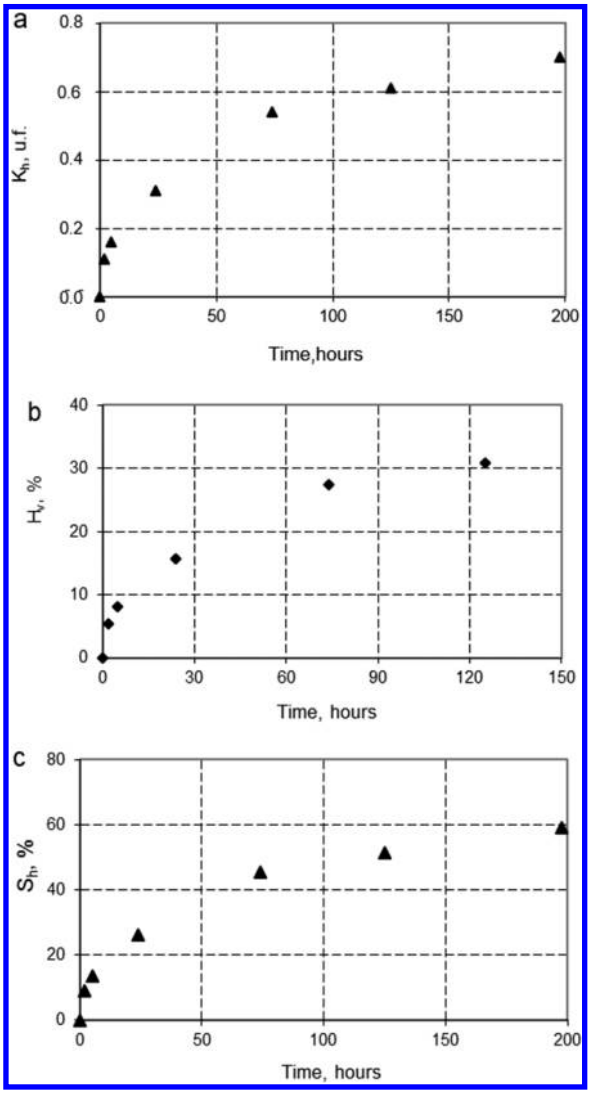

Figure 6. Pore methane hydrate formation in frozen sand-1 (W = 22%; n = 0.60) at t = −5 ± 1 °C: (a) time-dependent fraction of water changed to hydrate (K_h, unit fraction), (b) volume content of hydrate (H_v, %), and (c) hydrate saturation (S_h, %).

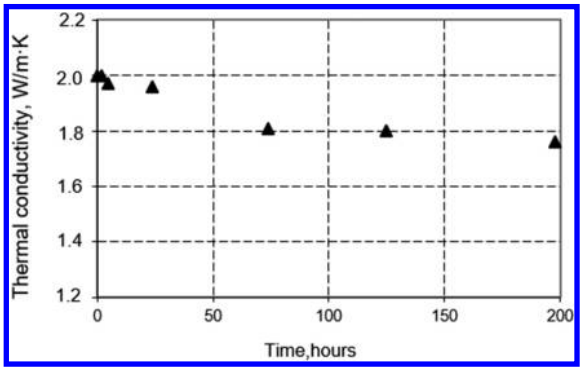

Figure 7. Time-dependent thermal conductivity of gas-saturated sand-1 (W = 22%; n = 0.60) during hydrate formation at t = −5 ± 1 °C.

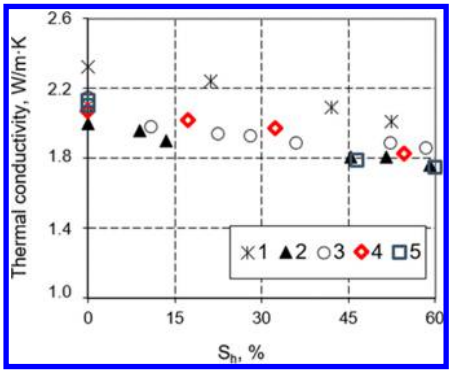

Figure 8. Thermal conductivity of sediments as a function of hydrate saturation (S_h), at t = −5 ± 1 °C: (1) sand-1, W = 19% and n = 0.40; (2) sand-1, W = 22% and n = 0.60; (3) sand-2, W = 15% and n = 0.38; (4) silty sand, W = 24% and n = 0.60; and (5) silty sand, W = 16% and n = 0.38.

Table 2. Methane Hydrate Formation upon Freezing of Residual Pore Water

			S_h (%)	
type of sediment	W (%)	ΔS_h (%)	before freezing	after freezing
sand-1	16	23	58	71
sand + 14% kaolin	15	28	62	79
silty sand	18	39	61	85
silty sand	16	52	52	79

the soil skeleton and release of dissolved gas produced new water−gas interfaces. The amount of hydrate additionally formed as a result of freezing mainly depends upon soil mineralogy, clay content, and water saturation.

The experiments show that thermal conductivity changed as the hydrate-saturated sediments froze (Figure 9). The phase change from water to ice caused a dramatic decrease in thermal conductivity of hydrate-bearing samples (Figure 9A), unlike the hydrate-barren samples in which thermal conductivity regularly became 15−20% higher (Figure 9B). The hydrate-bearing

DOI: 10.1021/acs.energyfuels.6b02726
Energy Fuels 2017, 31, 5246−5254

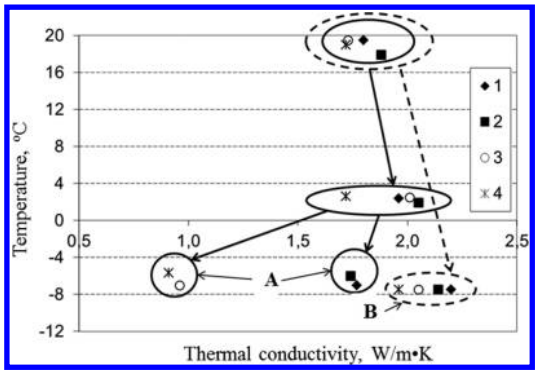

Figure 9. Variations in thermal conductivity of gas-saturated sediments upon cooling (to +2 °C) and freezing: (A) hydrate-bearing samples after freezing and (B) frozen hydrate-barren samples. Solid and dash lines correspond to samples saturated with gases that can and cannot form hydrates (methane and nitrogen, respectively): (1) sand-1, W = 16%; (2) sand + 14% kaolin, W = 15%; (3) silt, W = 18%; and (4) silt, W = 16%.

samples were of two groups: sand, including that mixed with finer grained material (clay), and silt (Figure 9A). The freezing-induced thermal conductivity reduction was 10% in sand but reached 50% in silt, from 1.96 to 1.77 W m^{-1} K^{-1} in hydrate-bearing sand-1 (W = 16%) and from 2.01 to 0.96 W m^{-1} K^{-1} in silt (W = 16%).

The decrease was proportional to additional hydrate formation (Figure 10): freezing led to a 23% increase of S_h

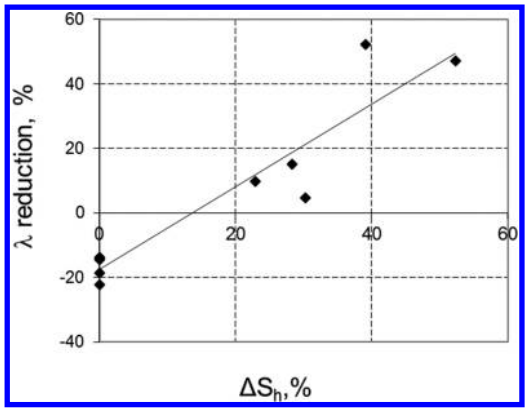

Figure 10. Correlation of freezing-induced thermal conductivity reduction and additional hydrate formation (ΔS_h).

in the sand-1 (W = 16%) sample that showed 10% thermal conductivity reduction but an almost 40% S_h growth in the silty sand sample (W = 18%), which became 50% less conductive.

Thus, the thermal conductivity may decrease dramatically in hydrate-saturated sediments exposed to further freezing, whereby the survived pore water freezes, as a result of related additional hydrate formation. This behavior of thermal conductivity may be due to structure and texture changes in freezing gas- and hydrate-bearing sediments. These are especially the effects of heaving or cracking of hydrate-saturated soil or the formation of pore hydrate on grain boundaries, with its thermal conductivity as low as 0.35 W m^{-1} K^{-1}.[18]

Such a dramatic thermal conductivity reduction in frozen hydrate-bearing samples was noted previously under non-equilibrium conditions.[27] The authors explained it by the formation of numerous microcracks and voids inside pore gas hydrates as a result of freezing and partial dissociation of pore hydrates by the self-preservation effect.

Effect of Thawing. To study the effect of thawing on the behavior of thermal conductivity, the frozen sand samples that were saturated with hydrate at t < 0 °C were heated to +2 ± 1 °C. The tests showed additional hydrate formation in sand (Table 3), as in the case of freezing, but unlike the latter case, it

Table 3. Thermal Conductivity and Hydrate Saturation of Frozen Hydrate-Bearing Sands upon Thawing (to +2 ± 1 °C) at Above-Equilibrium Methane Pressure

		S_h (%)		thermal conductivity (W m^{-1} K^{-1})	
type of sediment	W (%)	before freezing	after freezing	before thawing	after thawing
sand-1	19	0.64	0.71	1.80	1.70
sand-2	15	0.57	0.61	1.86	1.76

did not exceed 10%. We likewise attributed faster hydrate generation upon thawing to deformation of soil skeleton and formation of new water−gas interfaces.[33] Additional hydrate formation upon thawing of hydrate-saturated sand was more intense in the initially water-saturated samples: 10 and 7% of additional hydrate formed in samples sand-1 and sand-2 with W = 19 and 15%, respectively.

As the frozen hydrate-bearing samples thawed, their thermal conductivity decreased, e.g., from 1.86 to 1.72 W m^{-1} K^{-1} or by 8% in sand-2 (W = 15%). Two main reasons of such reduction are (i) the thermal conductivity difference between pore ice and water and (ii) the increase of hydrate saturation.

Thus, both freezing and thawing cause thermal conductivity reduction in frozen soil saturated with methane hydrate at above-equilibrium pressures.

Structure and Texture Changes Associated with Hydrate Formation in Gas-Saturated Sediments. For the reported data on thermal conductivity variations associated with hydrate formation in the experimental conditions of low positive and negative temperatures, freezing and thawing indicate that this behavior is mostly controlled by phase transitions in pore fluids and by structure and texture changes in main sample constituents. Early, Waite et al.[40] proposed several similar models for explanation variations of mechanical and seismic properties of sediments with different hydrate saturation at a temperature above 0 °C.

Proceeding from the experiment results, the structure and texture changes during hydrate formation in gas-saturated sediments can be described with two models of pore space changes: freezing of samples saturated with hydrate at t > 0 °C (model 1) and thawing of samples saturated with hydrate at t < 0 °C (model 2).

Model 1 includes several stages corresponding to different states of the samples (Figure 11): initial state before hydrate formation, cooling before hydrate formation, hydrate formation at S_h > 50%, and the state after freezing.

Initially, before hydrate formation, the pores are partly filled with water, which is in equilibrium with the hydrate-forming gas at pressures below equilibrium for the system "water−gas−hydrate" (Figure 11A). Then, as the system cools to the below-equilibrium temperature, rapid hydrate formation begins mainly along water−gas interfaces, while the pore space does not change much (Figure 11B). Thermal conductivity remains the same because its values for hydrate and pore water are similar.

DOI: 10.1021/acs.energyfuels.6b02726
Energy Fuels 2017, 31, 5246−5254

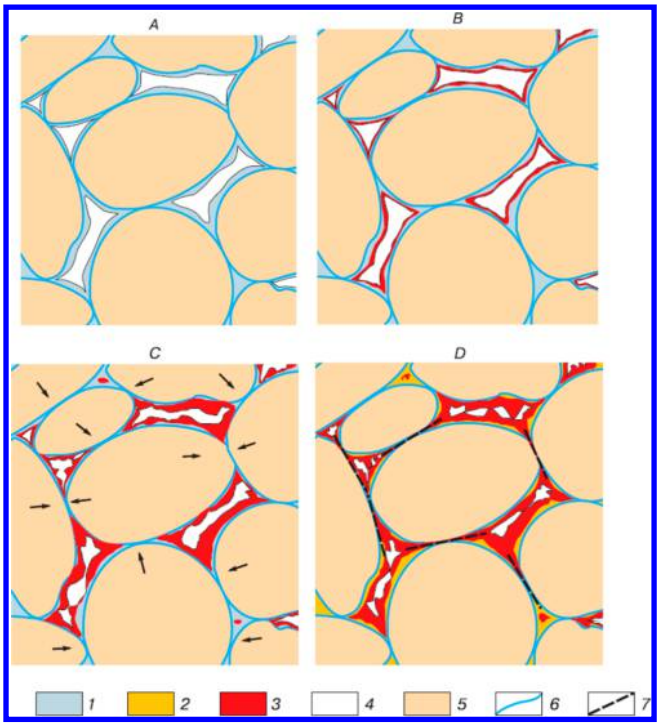

Figure 11. Pore-space changes in gas-saturated sediments exposed to hydrate formation at low positive temperatures (t > 0 °C) and freezing. Stages: (A) initial (before hydrate formation), (B) early pore hydrate formation, (C) hydrate formation at K_h > 0.40, and (D) freezing of the hydrate-bearing sample, with (1) water, (2) ice, (3) hydrate, (4) gas, (5) mineral grains, (6) bound water, and (7) cracks.

As hydrate saturates more than 50% of the total pore space, local migration and redistribution of pore water cause changes to the sample structure. Namely, water in films between particles moves inward toward the pores, closer to the water–gas interfaces, where hydrate is forming. Such local pore water migration during hydrate formation in porous media was discussed by Chaouachi et al.[41] As a result of the local redistribution of pore water, particles may become more tightly packed and saturation will increase. This affects the thermal contacts in the hydrate-bearing sediment (Figure 11C) expressed as an increase in thermal conductivity.

Freezing induces additional hydrate formation as the residual pore water freezes. The process can be accompanied by the formation of pore hydrate or ice, cracking, and hydrate formation on boundaries of grains or aggregates. The ensuing embrittlement of pore hydrate and ice and loosening of contacts between particles (Figure 11D) may account for the freezing-related thermal conductivity decrease observed in the experiments. A similar dramatic reduction of thermal conductivity in frozen hydrate-saturated samples at non-equilibrium conditions was reported previously.[27] The low thermal conductivity was explained in the cited paper by growth of microcracks and voids in porous hydrate-bearing soil that resulted from freezing and partial dissociation of pore hydrate during self-preservation.

In this case, it can be helpful to correlate frozen soils and gas hydrate-bearing sediments, in which the structural and textural features are poorly investigated. The proposed formation of microcracks in hydrate-bearing sediments exposed to freezing is similar to that in frozen sediments exposed to further cooling studied by Yershov[42] and Chuvilin and Yazynin.[43]

Model 2, for the pore space changes during hydrate saturation at t < 0 °C and subsequent thawing of soil samples, likewise includes several stages (Figure 12): before, in the

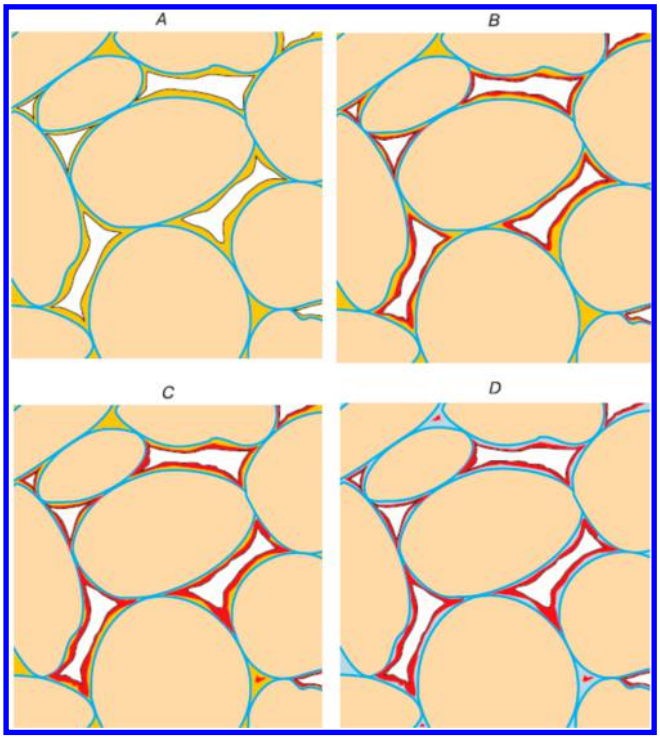

Figure 12. Pore-space changes in gas-saturated sediments exposed to hydrate formation at t < 0 °C and thawing. Stages: (A) initial (before hydrate formation), (B) early pore hydrate formation, (C) hydrate formation at S_h > 50%, and (D) thawing of the frozen hydrate-bearing sample, with symbols the same as in Figure 11.

beginning, and during hydrate formation (S_h > 50%) and during thawing. Before hydrate formation, the sediments have gas- and ice-saturated porosity at a gas pressure below equilibrium (Figure 12A). Hydrate formation begins as the gas pressure exceeds equilibrium, and pore ice converts to hydrate (Figure 12B). Pore gas hydrate expands from the surface inward toward the pore ice along cracks and structure defects. Then, as progressively greater amounts of ice change to hydrate, the hydrate formation process attenuates, at S_h > 50% (Figure 12C). The changes in the pore ice/hydrate ratio during hydrate formation at t < 0 °C decrease thermal conductivity of frozen samples because the share of the more conductive ice component with 2.23 W m^{-1} K^{-1} decreases, while the 4 times less conductive (0.6 W m^{-1} K^{-1}) hydrate component increases.

Further on, as the conversion of pore ice into hydrate slows at S_h > 50%, thermal conductivity decreases only slightly. Thawing of hydrate-bearing soils under a pressure below equilibrium causes melting of the residual pore ice, producing new water–gas interfaces, and, thus, induces additional hydrate formation (Figure 12D). Thawing of frozen hydrate-bearing sediments reasonably reduces their thermal conductivity because the share of the low conductive component in the pore space increases.

The suggested models may be useful for geomechanical and thermal simulation of methane recovery from gas hydrate reservoirs. The models take into account features of hydrate-saturated sediments at different thermobaric conditions.

DOI: 10.1021/acs.energyfuels.6b02726
Energy Fuels 2017, 31, 5246–5254

CONCLUSION

A new experimental technique is suggested to study the thermal conductivity of gas-, water-, hydrate-, and ice-bearing sediments under different temperatures and pressures at a gas pressure to 7 MPa. The obtained thermal conductivity estimates are accurate to 7%, at a confidence of 0.95, with a random measurement error no higher than 4%.

The reported experimental results have demonstrated the behavior of thermal conductivity in gas-saturated sediments, which experience hydrate formation in the conditions of low positive and negative temperatures, freezing, and thawing.

During hydrate formation at $t > 0$ °C, thermal conductivity changed insignificantly (within 2−3%) when less than a half of the total pore space was saturated with gas hydrate ($S_h < 50\%$) but increased notably (for 14% in silt with $W = 18\%$) as the saturation reached $S_h = 61\%$.

Thermal conductivity became lower upon hydrate formation at $t < 0$ °C to 22% in the sand sample of $W = 19\%$ at $S_h = 52\%$.

Both freezing and thawing of samples saturated with hydrate at low positive and negative temperatures, respectively, led to thermal conductivity reduction: about 10% for sand and 50% for silty sand. The observed thermal conductivity behavior results from pore space changes associated with additional hydrate formation, as explained in two models. These models can be used for reference in geomechanical and thermal simulations of gas hydrate reservoirs, taking into account the conditions of pore hydrate formation, with implications for methane recovery.

AUTHOR INFORMATION

Corresponding Author

*Telephone: +7-495-9391927. E-mail: chuviline@msn.com and/or e.chuvilin@skoltech.ru.

ORCID

Evgeny Chuvilin: 0000-0003-1173-546X

Notes

The authors declare no competing financial interest.

ACKNOWLEDGMENTS

This research was supported by the Russian Science Foundation (Grant 16-17-00051).

REFERENCES

(1) Sloan, E. D. *Clathrate Hydrates of Natural Gases*, 2nd ed.; Marcel Dekker: New York, 1998.

(2) Max, M. D. *Natural Gas Hydrate in Oceanic and Permafrost Environments*; Kluwer Academic Publishers: Boston, MA, 2000.

(3) Sloan, E. D.; Koh, C. A. *Clathrate Hydrates of Natural Gases*, 3rd ed.; CRC Press: Boca Raton, FL, 2008.

(4) Yakushev, V. S.; Chuvilin, E. M. *Cold Reg. Sci. Technol.* **2000**, *31*, 189−197.

(5) Chuvilin, E. M.; Yakushev, V. S.; Perlova, E. V. *Polarforschung* **1998**, 215−219.

(6) Romanovsky, N. N. *Cryogenesis of Lithosphere*; Moscow State University (MSU): Moscow, Russia, 1993 (in Russian).

(7) Makogon, Yu. F.; Trebin, F. A.; Trofimuk, A. A.; Tsarev, V. P.; Cherskiy, N. V. *Rep. Acad. Sci. USSR* **1972**, *196*, 197−200.

(8) Johnson, A. H. *Fire Ice* **2011**, *11* (2), 1−5.

(9) Boswell, R.; Collett, T. S. *Energy Environ. Sci.* **2011**, *4*, 1206−1215.

(10) Ohgaki, K.; Takano, K.; Sangawa, H.; Matsubara, T.; Nakano, S. *J. Chem. Eng. Jpn.* **1996**, *29*, 478−483.

(11) Tang, L. G.; Xiao, R.; Huang, C.; Feng, Z. P.; Fan, S. S. *Energy Fuels* **2005**, *19*, 2402−2407.

(12) Ye, Y.; Liu, C. *Natural Gas Hydrates. Experimental Techniques and Their Applications*; Springer: New York, 2013.

(13) Max, M. D.; Johnson, A. H. *Exploration and Production of Oceanic Natural Gas Hydrate*; Springer: New York, 2016.

(14) Warzinski, R. P.; Gamwo, I. K.; Rosenbaum, E. J.; Myshakin, E. M.; Jiang, H.; Jordan, K. D.; English, N. J.; Shaw, D. W. *Proceedings of the 6th International Conference on Gas Hydrates (ICGH 2008)*; Vancouver, British Columbia, Canada, July 6−10, 2008.

(15) Stoll, R. D.; Bryan, G. M. *J. Geophys. Res.* **1979**, *84*, 1629−1634.

(16) Huang, D.; Fan, S. *J. Chem. Eng. Data* **2004**, *49*, 1479−1482.

(17) Waite, W. F.; Stern, L. A.; Kirby, S. H.; Winters, W. J.; Mason, D. H. *Geophys. J. Int.* **2007**, *169*, 767−774.

(18) Rosenbaum, E. J.; English, N. J.; Johnson, J. K.; Shaw, D.; Warzinski, R. P. *J. Phys. Chem. B* **2007**, *111*, 13194−13205.

(19) Groysman, A. G. *Thermophysical Properties of Gas Hydrates*; Nauka: Novosibersk, Russia, 1985.

(20) Asher, G. B. Development of computerized thermal conductivity measurement system utilizing the transient needle probe technique: An application to hydrates in porous media. Ph.D. Thesis, Colorado School of Mines, Golden, CO, 1987.

(21) Fan, S.; Huang, D.; Liang, D. *Proceedings of the 5th International Conference on Gas Hydrates (ICGH 2005)*; Trondheim, Norway, June 13−16, 2005; Vol. 2, pp 668−676.

(22) Duchkov, A. D.; Manakov, A. Yu.; Kazantsev, S. A.; Permyakov, M. E.; Ogienko, A. G. *Dokl. Earth Sci.* **2006**, *409* (5), 732−735.

(23) Muraoka, M.; Susuki, N.; Yamaguchi, H.; Tsuji, T.; Yamamoto, Y. *Energy Fuels* **2015**, *29* (3), 1345−1351.

(24) Yang, L.; Zhao, J.; Wang, B.; Liu, W.; Yang, M.; Song, Y. *Fuel* **2016**, *179*, 87−96.

(25) Wright, J. F.; Nixon, F. M.; Dallimore, S. R.; Henninges, J.; Cote, M. M. In *Mallik 5L-38 Gas Hydrate Production Research Well*; Dallimore, S. R., Collett, T. S., Eds.; Geological Survey of Canada: Ottawa, Ontario, Canada, 2005; Bulletin 585, pp 1−5.

(26) Muraoka, M.; Ohtake, M.; Susuki, N.; Yamamoto, Y.; Suzuki, K.; Tsuji, T. *J. Geophys. Res. Solid Earth.* **2014**, *119*, 8021−8033.

(27) Bukhanov, B. A.; Chuvilin, E. M.; Guryeva, O. M.; Kotov, P. I. *Proceedings of the 9th International Conference on Permafrost (ICOP)*; Fairbanks, AK, June 28−July 3, 2008; pp 205−209.

(28) Ershov, E. D.; Lebedenko, Yu.P.; Chuvilin, E. M.; Istomin, V. A.; Yakushev, V. S. *Rep. Acad. Sci. USSR* **1991**, *321* (4), 788−791 (in Russian).

(29) Stern, L.; Circone, S.; Kirby, S. H.; Durham, W. *J. Phys. Chem. B* **2001**, *105*, 1756−1762.

(30) Bertasi, M.; Bigolaro, G.; De Ponte, F. Fibrous Insulating Materials as Standard Reference Materials at Low Temperatures. In *Thermal Transmission Measurements of Insulation*; Tye, R. P., Ed.; American Society for Testing and Materials: Philadelphia, PA, 1978; ASTM STP660, pp 7−29, DOI: 10.1520/STP35734S.

(31) Chuvilin, E. M.; Bukhanov, B. A.; Brovka, G. P. *Proceedings of the 7th Canadian Permafrost Conference*; Québec City, Québec, Canada, Sept 20−23, 2015; ABS_305, pp 1−6.

(32) Degenne, M.; Klarsfeld, S.; Barthe, M. P. Measurement of the Thermal Resistance of Thick Low-Density Mineral Fiber Insulation. In *Thermal Transmission Measurements of Insulation*; Tye, R.P., Ed.; American Society for Testing and Materials: Philadelphia, PA, 1978; ASTM STP660, pp 130−144, DOI: 10.1520/STP35740S.

(33) Chuvilin, E. M.; Kozlova, E. V. *Proceedings of the 5th International Conference on Gas Hydrates (ICGH 2005)*; Trondheim, Norway, June 13−16, 2005; Vol. 5, pp 1562−1567.

(34) Takeya, S.; Uchida, T.; Kamata, Y.; Nagao, J.; Kida, M.; Minami, H.; Sakagami, H.; Hachikubo, A.; Takahashi, N.; Shoji, H.; Khlystov, O.; Grachev, M.; Soloviev, V. *Angew. Chem., Int. Ed.* **2005**, *44*, 6928−6931.

(35) Rempel, A. W.; Buffett, B. A. *J. Geophys. Res.* **1997**, *102*, 10151−10164.

(36) Chuvilin, E. M.; Lupachik, M. V.; Guryeva, O. M. In *Physics and Chemistry of Ice*; Furukawa, Y., Sazaki, G., Uchida, T., Watanabe, N., Eds.; Hokkaido University Press: Sapporo, Japan, 2011; pp 127−132.

DOI: 10.1021/acs.energyfuels.6b02726
Energy Fuels 2017, 31, 5246−5254

(37) Kuhs, W. F.; Klapproth, A.; Gotthardt, F.; Techmer, K.; Heinrichs, T. *Geophys. Res. Lett.* **2000**, *27* (18), 2929−2932.
(38) Wang, X.; Schultz, A. J.; Halpern, Yu. *Proceedings of the 4th International Conference on Gas Hydrates (ICGH 2002)*; Yokohama, Japan, May 19−23, 2002; pp 455−460.
(39) Staykova, D. K.; Kuhs, W. F.; Salamatin, A.; Hansen, T. *J. Phys. Chem. B* **2003**, *107*, 10299−10311.
(40) Waite, W. F.; Santamarina, J. C.; Cortes, D. D.; Dugan, B.; Espinoza, D. N.; Germaine, J.; Jang, J.; Jung, J. W.; Kneafsey, T. J.; Shin, H.; Soga, K.; Winters, W. J.; Yun, T. S. *Rev. Geophys.* **2009**, *47* (4), 1−38.
(41) Chaouachi, M.; Falenty, A.; Sell, K.; Enzmann, F.; Kersten, M.; Haberthur, D.; Kuhs, W. F. *Geochem., Geophys., Geosyst.* **2015**, *16*, 1711−1722.
(42) Yershov, E. D. *General Geocryology*; Cambridge University Press: Cambridge, U.K., 1998.
(43) Chuvilin, E. M.; Yazynin, O. M. *Proceedings of the 5th International Permafrost Conference*; Trondheim, Norway, Aug 2−5, 1988; pp 320−323.

DOI: 10.1021/acs.energyfuels.6b02726
Energy Fuels 2017, 31, 5246−5254